AFOSR - TR - 76 - 0754

FC

03

SC579.3IR

ANALYSIS OF ULTRASONIC WAVE SCATTERING FOR CHARACTERIZATION OF DEFECTS IN SOLIDS

Second Annual Interim Report
for the
Period 1975 March 16 to 1976 March 15

AFOSR Contract No. F44620-74-C-0057

Prepared for

Air Force Office of Scientific Research
Bolling Air Force Base
Washington, D. C. 20332

by

E. Richard Cohen
Principal Investigator

Science Center
Rockwell International

Qualified requestors may obtain additional copies from the Defense Documentation Center, all others should apply to the National Technical Information Center.

Unclassified

SECURITY CLASSIFICATION OF THIS PAGE (When Data Entered)

REPORT DOCUMENTATION PAGE	READ INSTRUCTIONS BEFORE COMPLETING FORM
1. REPORT NUMBER: AFOSR - TR - 76 - 0754	2. GOVT ACCESSION NO. / 3. RECIPIENT'S CATALOG NUMBER
4. TITLE (and Subtitle): Analysis of Ultrasonic Wave Scattering for Characterization of Defects in Solids.	5. TYPE OF REPORT & PERIOD COVERED: Interim, 75 March 16-76 March 15
	6. PERFORMING ORG. REPORT NUMBER: SC579.3IR
7. AUTHOR(s): E. Richard Cohen	8. CONTRACT OR GRANT NUMBER(s): F44620-74-C-0057
9. PERFORMING ORGANIZATION NAME AND ADDRESS: Science Center, Rockwell International Corp., 1049 Camino Dos Rios, Thousand Oaks, CA 91360	10. PROGRAM ELEMENT, PROJECT, TASK AREA & WORK UNIT NUMBERS: 681307, 9782-05, 61102F
11. CONTROLLING OFFICE NAME AND ADDRESS: Air Force Office of Scientific Research/NA, Building 410, Bolling Air Force Base, D.C. 20332	12. REPORT DATE: May 1976
	13. NUMBER OF PAGES: 40
14. MONITORING AGENCY NAME & ADDRESS (if different from Controlling Office): Annual Interim rept. no. 2, 16 Mar 75 - 15 Mar 76	15. SECURITY CLASS. (of this report): Unclassified
	15a. DECLASSIFICATION/DOWNGRADING SCHEDULE

16. DISTRIBUTION STATEMENT (of this Report)

Approved for public release; distribution unlimited

(12) 39 p.

17. DISTRIBUTION STATEMENT (of the abstract entered in Block 20, if different from Report)

(16) AF-9782 (17) 9782-05

18. SUPPLEMENTARY NOTES

19. KEY WORDS (Continue on reverse side if necessary and identify by block number)

Ultrasonics; elastic waves; defects in solids; voids; scattering; angular distribution; non-destructive testing (NDT); tungsten carbide; Ti-6Al-4V; integral equations; Born approximation

20. ABSTRACT (Continue on reverse side if necessary and identify by block number)

Measurements have been carried out on scattering of ultrasonic waves by a solid spherical inclusion (tungsten carbide) in titanium alloy. Both direct scattering and mode-converted scattering angular distributions were measured for both shear and compressional incident waves. The scattering from an arbitrary shape was expressed in terms of an integral equation from which an improved Born approximation was developed. In this formulation, the Born approximation reduces to the Rayleigh limit at low frequencies.

DD FORM 1 JAN 73 1473 EDITION OF 1 NOV 65 IS OBSOLETE

Unclassified 389 949

SECURITY CLASSIFICATION OF THIS PAGE (When Data Entered)

AB

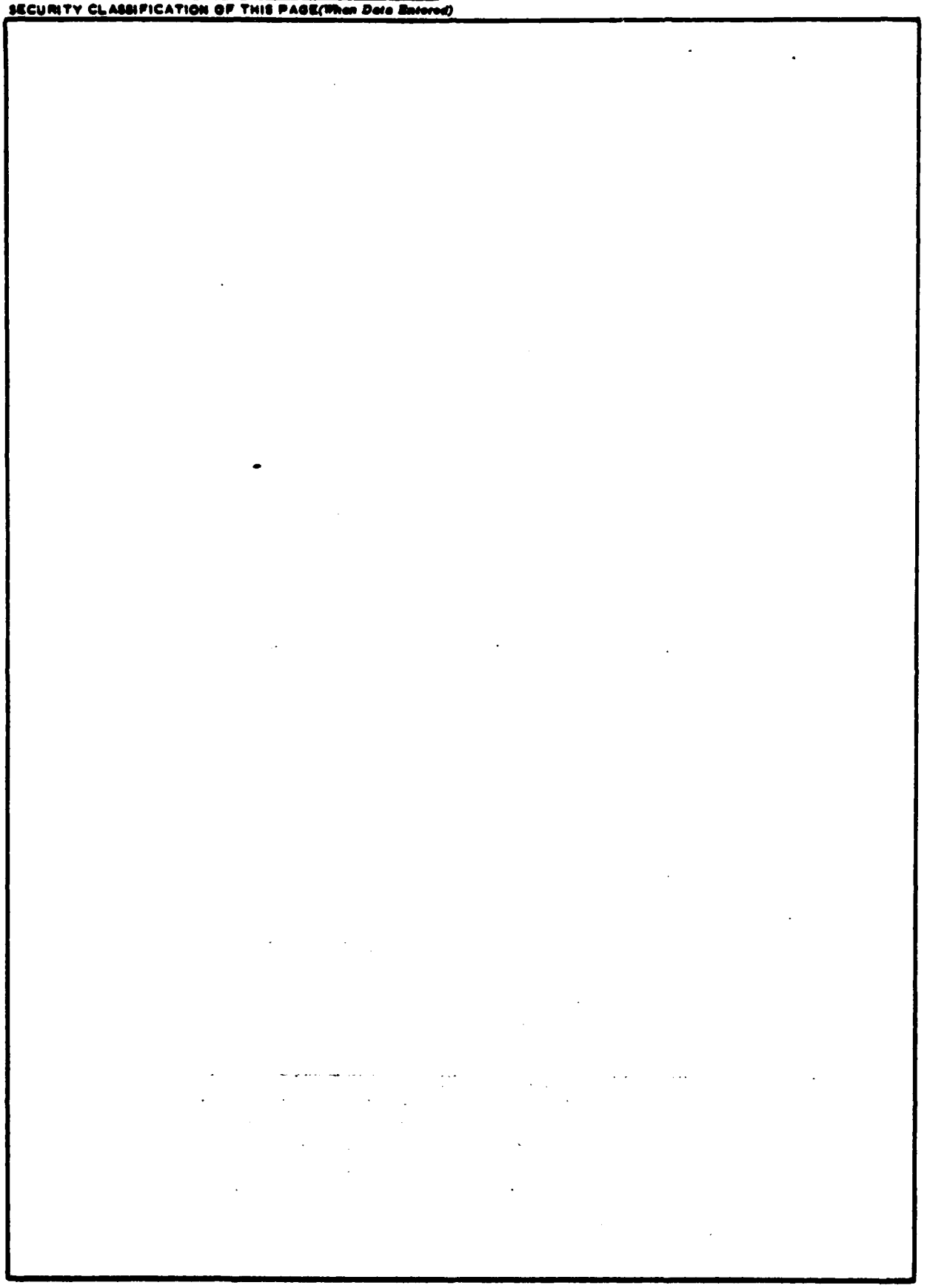

I. INTRODUCTION

This report is the second annual interim report on contract F44620-74-C-0057 to study the application of ultrasonic acoustic wave scattering to the detection, identification and characterization of defects in solids. The contract was initiated on 1 February 1974 has entailed approximately one man-year of effort equally divided between the theoretical analysis of the scattering process and an experimental program to verify its validity and measurability.

II. SUMMARY OF PROGRESS

1. Scattering of Acoustic Waves by Spherical Obstacles and Voids

The specific goal of the present program is the characterization of the scattering of acoustic waves by ellipsoidal obstacles. However, in order to verify the experimental techniques and to develop the necessary theoretical basis, the initial task chosen was the review of the existing calculations of scattering by spheres and the verification of the experimental technique using spherical cavities and spherical inclusions embedded in a solid matrix.[1]

The results of this work have been partially reported in a paper submitted to the "Journal of the Acoustical Society of America." The abstract of this paper is presented here:

a. "Scattering of Longitudinal Waves Incident on a Spherical Cavity in a Solid," B. R. Tittmann and E. Richard Cohen

Experimental data are compared with theoretical calculations for the scattering of ultrasonic pulses from a single spherical cavity embedded in a metallic solid. Except at high frequencies, the data are in reasonable agreement with theory, bearing out the notable features predicted for the angular dependence and the mode conversion between

longitudinal and transverse waves. At high frequencies the disagreement can be accounted for by the lack of monochromicity in the ultrasonic pulse. The experiments were typically carried out in the regime where the wavelength is approximately equal to the size of the spherical cavity (0.8 mm) on samples of diffusion-bonded Ti-6% Al-4%V.

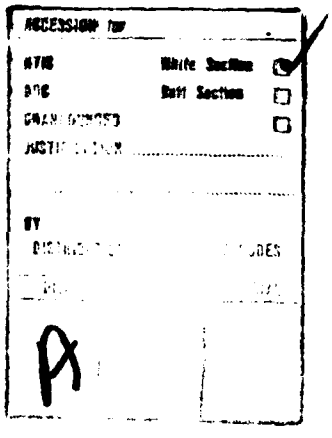

2. Scattering by a Spherical Inclusion

During this past year the experimental portion of the program has concentrated on the measurement of the scattering characteristics of the tungsten carbide inclusion. Sample preparation was carried out in a manner similar to that associated with the preparation of the 800μm spherical cavity except that a commercially obtained tungsten carbide ball with a nominal diameter of 1/32" (794μm) was inserted into the cavity at the center of the sample prior to diffusion bonding. As before, the sample was given a polygonal geometry with 14 flat faces each just under 0.5" wide.

The experiments for incident longitudinal waves were carried out as before with a matched pair of Panametrics broadband transducers. The three pairs of transducers were designated as 2.25 MHz, 5 MHz and 10 MHz, but because of the broadband character, with a Q of approximately 5, waveform synthesis was required.[2] The 2.25 MHz transducers showed a response characteristic with a full width at half maximum of 0.8 MHz. The peak response of the 5 MHz transducers was at 4.5 MHz with a full width at half maximum of 1.9 MHz and for the 10 MHz transducers the peak response was at 7.4 MHz with a full width at half maximum of 2.6 MHz (Fig. 1). On the other hand, the shear wave transducers used for generating and receiving transversely polarized waves were high Q devices with well-defined monochromatic response curves which were within 1 to 1.5% of 2.5 MHz, 5.0 MHz and 10.0 MHz, respectively.

The results for incident longitudinal waves are shown in Figs. 2, 3, and 4. The angular distribution for L→L scattering was calculated for 2.25 MHz. The synthesized curve using the measured response of Fig. 1 was essentially identical to this curve. The curve marked L→T was calculated for a frequency of 2.5 MHz since this is the frequency to which the receiver responds. In

Fig. 3 the mode-converted angular distribution is similarly calculated for a frequency of 5.0 MHz, while the direct scattered curve (L→L) is calculated from the spectral synthesis (solid curve). Also shown are monochromatic 4 and 5 MHz curves. These indicate the sensitivity of the angular distribution to frequency or to size of the scatterer as well as the averaging effect of frequency synthesis. In Fig. 4 the 10 MHz monochromatic curve shows a great deal of structure, in particular, the surprisingly sharp dip at 92° in the mode-converted scattered shear wave. The directly-scattered 10 MHz curve (L→L) is indicated although it has little bearing to the experimental data since there is little 10 MHz content in the pulse. The 7.4 MHz monochromatic curve (corresponding to the peak frequency of the broadband pulse) is much closer to the synthesized curve which shows, as is to be expected, rather broad features with no sharp detail.

The experimental data was fitted to these curves by choosing an arbitrary normalization in order to give the best fit. The lack of agreement between the synthesized calculation and the data for L→L scattering in Fig. 4 may be the result of scatter from a secondary metallurgical phase which would become more important at higher frequencies. One possible source of error in the mode-converted cases (L→T) is the unfortunate mismatch between the transmitter frequency which peaks at 7.4 MHz and has a distribution with a mean frequency of 7.26 MHz with a standard deviation of 1.16 MHz; there is thus very little power at 10 MHz for the receiver to respond to.

Experiments with incident shear waves were carried out with shear-cut quartz plates which were bonded to the faces of the sample with low-melting-point wax and which could be polarized either parallel or perpendicular to the scattering plane. The results are presented in Figs. 5, 6 and 7. The angular distribution for the mode-converted scattered compressional wave

Fig. 3 the mode-converted angular distribution is similarly calculated for a frequency of 5.0 MHz, while the direct scattered curve (L→L) is calculated from the spectral synthesis (solid curve). Also shown are monochromatic 4 and 5 MHz curves. These indicate the sensitivity of the angular distribution to frequency or to size of the scatterer as well as the averaging effect of frequency synthesis. In Fig. 4 the 10 MHz monochromatic curve shows a great deal of structure, in particular, the surprisingly sharp dip at 92° in the mode-converted scattered shear wave. The directly-scattered 10 MHz curve (L→L) is indicated although it has little bearing to the experimental data since there is little 10 MHz content in the pulse. The 7.4 MHz monochromatic curve (corresponding to the peak frequency of the broadband pulse) is much closer to the synthesized curve which shows, as is to be expected, rather broad features with no sharp detail.

The experimental data was fitted to these curves by choosing an arbitrary normalization in order to give the best fit. The lack of agreement between the synthesized calculation and the data for L→L scattering in Fig. 4 may be the result of scatter from a secondary metallurgical phase which would become more important at higher frequencies. One possible source of error in the mode-converted cases (L→T) is the unfortunate mismatch between the transmitter frequency which peaks at 7.4 MHz and has a distribution with a mean frequency of 7.26 MHz with a standard deviation of 1.16 MHz; there is thus very little power at 10 MHz for the receiver to respond to.

Experiments with incident shear waves were carried out with shear-cut quartz plates which were bonded to the faces of the sample with low-melting-point wax and which could be polarized either parallel or perpendicular to the scattering plane. The results are presented in Figs. 5, 6 and 7. The angular distribution for the mode-converted scattered compressional wave

(T→L) is the same as the mode-converted scattered shear wave from incident compressional waves (L→T). This "reciprocity" in the scattering is discussed more fully in Section II.3 below.

The curves marked $T \rightarrow T_{\parallel}$ and $T \rightarrow T_{\perp}$ in Figs. 5, 6 and 7 represent the amplitudes of the scattered shear wave when the plane of polarization of the incident shear wave is parallel and perpendicular to the scattering plane. The measurements were made in these two orientations. In general, when the scattering plane is oriented at an angle ϕ to the plane of incident polarization, the scattered shear wave is elliptically polarized; the amplitude of the shear wave in the scattering plane is

$$A_{\parallel}(R,\theta,\phi) = \frac{a}{R} A_{T \rightarrow T_{\parallel}}(\theta)\cos\phi \qquad (2.1)$$

and the amplitude of the shear wave perpendicular to that plane is

$$A_{\perp}(R,\theta,\phi) = \frac{a}{R} A_{T \rightarrow T_{\perp}}(\theta)\sin\phi \quad . \qquad (2.2)$$

The measurements at 5 MHz however showed the cross-polarized wave at perpendicular scattering to have an appreciable amplitude. This is not understood at this time; it may be the result of scattering by the metallurgical second phase in the titanium alloy. This background scattering may also be the cause of the lack of qualitative agreement between theory and experiment observed in the shear wave scattering at 5 MHz, and requires further investigation.

3. Reciprocity

In the course of the measurements of mode-conversion in scattering from spherical cavities and inclusions, it was recognized that the angular distribution for the mode-converted component is the same for the shear wave scattered from an incident compressional wave and for the compressional wave scattered from an incident shear wave. Thus, in Figs. 5, 6 and 7, the curves labeled T→L differ only by a constant factor from those in 2, 3 and 4 labeled L→T.

This result had not been anticipated but is contained in the analytic expressions for the scattering amplitudes. The amplitudes of the scattering by a spherical scatterer are given by expressions of the following form:

For incident compressional wave, normalized to unit amplitude for the displacement in the incident wave[3]:

$$u_r = \frac{ie^{-ikr}}{kr}\sum(2n+1)A_nP_n(\cos\theta) \tag{3.1}$$

$$u_\theta = \frac{ie^{-i\kappa r}}{\kappa r}\sum(2n+1)B_nP_n^1(\cos\theta) \tag{3.2}$$

For incident shear waves, similarly normalized:

$$u_r = -\frac{ie^{-ikr}}{kr}\sum\frac{2n+1}{n(n+1)}E_nP_n^1(\cos\theta) \tag{3.3}$$

$$u_\theta = \frac{ie^{-i\kappa r}}{\kappa r}\cos\phi\sum\frac{2n+1}{n(n+1)}\left[K_n\frac{P_n^1(\cos\theta)}{\sin\theta} + F_n\frac{dP_n^1(\cos\theta)}{d\theta}\right] \tag{3.4}$$

$$u_\phi = \frac{ie^{-i\kappa r}}{\kappa r}\sin\phi\sum\frac{2n+1}{n(n+1)}\left[K_n\frac{dP_n^1(\cos\theta)}{d\theta} + F_n\frac{P_n^1(\cos\theta)}{\sin\theta}\right] \tag{3.5}$$

By direct evaluation of the equations which define the constants in these expansions[3] we can show that

$$E_n = n(n+1)(k/\kappa)^3 B_n \quad . \tag{3.6}$$

This result can be obtained without explicitly evaluating the complete expressions for E_n and B_n. It had previously been shown to hold for the Rayleigh limit, $ka \ll 1$, but is now established for arbitrary values of ka.

Thus we have

$$u_r(\text{shear})/u_\theta(\text{compr.}) = u(T\to L)/u(L\to T) = k^2/\kappa^2 \tag{3.7}$$

and the differential scattering cross sections $\sigma_{T\to L}(\theta)$ and $\sigma_{L\to T}(\theta)$ are also in the same ratio

$$\sigma_{T\to L}(\theta)/\sigma_{L\to T}(\theta) = k^2/\kappa^2 = \frac{\mu}{\lambda+2\mu} \quad . \tag{3.8}$$

This result in fact appears to be a special case of a much more general reciprocity theorem valid for a scatterer of arbitrary shape in an elastic medium, which follows from general arguments of symmetry and invariance. If we consider an arbitrary shape (Fig. 8) with an incident plane wave of polarization p and propagation vector $\underline{K}_I$, the scattered wave amplitude with polarization q and propagation vector $\underline{K}_S$ can be written as $K_S^2 f_{pq}(\underline{K}_I, \underline{K}_S)$ and reciprocity is contained in the invariance of f to the interchange of $p \leftrightarrow q$ and simultaneously $\underline{K}_I \leftrightarrow -\underline{K}_S$, i.e.,

$$f_{pq}(\underline{K}_I, \underline{K}_S) = f_{qp}(-\underline{K}_S, -\underline{K}_I) \tag{3.9}$$

For the sphere the additional symmetry is such that $f_{pq}(\underline{K}_I, \underline{K}_S)$ depends only on the angle of scattering; i.e., on $\underline{K}_I \cdot \underline{K}_S$ and not on the orientation of the vectors individually.

The reciprocity theorem in its most general form may easily be established for an arbitrary elastic medium.[4] We consider a region of space $\mathcal{R}$ with density ρ and elastic coefficients C_{mnps} (both functions in general of position). The elastic displacements at point $\underline{r}$ produced by a unit delta-function force of frequency ω applied in the j-direction at point $\underline{r}_1$ is a solution of the equation*

$$\left(C_{mnps}(r)u^j_{s,p}(\underline{r};\underline{r}_1)\right)_{,n} + \rho(\underline{r})\omega^2 u^j_m(\underline{r};\underline{r}_1) + \delta_{jm}\delta(\underline{r}-\underline{r}_1) = 0 \qquad (3.10)$$

Similarly we write

$$\left(C_{mnps}(r)u^q_{s,p}(\underline{r};\underline{r}_2)\right)_{,n} + \rho(\underline{r})\omega^2 u^q_m(\underline{r};\underline{r}_2) + \delta_{qm}\delta(\underline{r}-\underline{r}_2) = 0 \qquad (3.11)$$

Now multiply the first equation by $u^q_m(\underline{r};\underline{r}_2)$, the second by $-u^j_m(\underline{r};\underline{r}_1)$, add and integrate over the region $\mathcal{R}$. Because of the symmetry of the elastic coefficients, $C_{mnps}(\underline{r}) = C_{psmn}(\underline{r}) = C_{nmps}(\underline{r})$, one obtains

$$\begin{aligned}\int_{\mathcal{R}} &\left(C_{mnps}(r)\left\{u^q_m(\underline{r};\underline{r}_2)u^j_{s,p}(\underline{r};\underline{r}_1) - u^j_m(\underline{r};\underline{r}_1)u^q_{s,p}(\underline{r};\underline{r}_2)\right\}\right)_{,n} dv \\ &= \int_S \Big[u^q_m(\underline{r};\underline{r}_2)C_{mnps}(\underline{r})u^j_{s,p}(\underline{r};\underline{r}_1) \\ &\qquad - u^j_m(\underline{r};\underline{r}_1)C_{mnps}u^q_{s,p}(\underline{r};\underline{r}_2)\Big] dS_n \\ &= -u^q_j(\underline{r}_1;\underline{r}_2) + u^j_q(\underline{r}_2;\underline{r}_1) \end{aligned} \qquad (3.12)$$

*We utilize the ordinary tensor notation in which summation is assumed on repeated indices and a comma indicates differentiation with respect to the following coordinate indices.

If the region $\mathcal{R}$ extends to infinity the displacements fall to zero at least as fast as $1/r$ and the surface integral vanishes. If the region $\mathcal{R}$ is finite we assume homogeneous boundary conditions such that either the displacements or the normal derivatives of the stresses vanish on the boundary surface and again the surface integral will vanish. We therefore obtain the reciprocity rule:

$$u_j^q(\underline{r}_1;\underline{r}_2) = u_q^j(\underline{r}_2;\underline{r}_1) \tag{3.13}$$

which states that the j-displacement at $\underline{r}_1$ due to a unit q-force at $\underline{r}_2$ is equal to the q-displacement at $\underline{r}_2$ resulting from a j-force at $\underline{r}_1$. Thus a receiver at $\underline{r}_2$ responding to waves with polarization q from a transmitter at $\underline{r}_1$ exciting displacements of polarization p will record the same signal when the transmitter and receiver are interchanged.

4. Integral Formulation of Scattering

As an alternative to the normal mode expansion which is so useful in spherical coordinates and whose extension to spheroidal coordinates involves serious computational problems, an integral formulation has also been explored, based on the utilization of Green's function for an elastic medium.

We consider an infinite medium of density $\rho'(\underline{r})$ and elastic constants $C'_{mnps}(\underline{r})$ such that for $r \to \infty$ the medium is homogeneous, isotropic and uniform with density ρ and elastic constants $C_{mnps} = \lambda\delta_{mn}\delta_{ps} + \mu(\delta_{mp}\delta_{ns} + \delta_{ms}\delta_{np})$. The elastic displacements with frequency ω in the medium are given by

$$\left(C'_{mnps}(\underline{r})u_{s,p}(\underline{r})\right)_{,n} + \rho'(\underline{r})\omega^2 u_m(\underline{r}) = 0 \tag{4.1}$$

We introduce the Green's function $G^j_m(\underline{r};\underline{r}_1)$ for the uniform medium which satisfies

$$C_{mnps}G^j_{s,pn}(\underline{r};\underline{r}_1) + \rho\omega^2 G^j_m(\underline{r};\underline{r}_1) + \delta_{jm}\delta(\underline{r}-\underline{r}_1) = 0 \tag{4.2}$$

The inhomogeneity of the medium is then defined by

$$\Delta C_{mnps}(\underline{r}) = C'_{mnps}(\underline{r}) - C_{mnps} \tag{4.3}$$

$$\Delta\rho(\underline{r}) = \rho'(\underline{r}) - \rho \tag{4.4}$$

In a manipulation similar to that in the previous section we obtain

$$\int_{\mathcal{R}} \Big\{ G_m^j(r;\underline{r}_1)\Big(C_{mnps}(\underline{r})u_{s,p}(\underline{r})\Big)_{,n} - u_m(\underline{r})C_{mnps}G^j_{s,pn}(\underline{r};\underline{r}_1) + \Delta\rho(\underline{r})G_m^j(r;\underline{r}_1)u_m(\underline{r})\Big\}dv = \begin{cases} u_j(\underline{r}_1) & \underline{r}_1\in\mathcal{R} \\ 0 & \underline{r}_1\notin\mathcal{R} \end{cases} \tag{4.5}$$

Then, for $\underline{r}_1\in\mathcal{R}$ one obtains

$$u_j(\underline{r}_1) = \int_S \Big[C'_{mnps}(\underline{r})G_m^j(\underline{r};\underline{r}_1)u_{s,p}(\underline{r}) - C_{mnps}u_m(\underline{r})G^j_{s,p}(\underline{r};\underline{r}_1)\Big]dS_n + \int\Big\{\Delta\rho(r)\omega^2G_m^j(\underline{r};\underline{r}_1)u_m(\underline{r}) - \Delta C_{mnps}(\underline{r})G^j_{s,p}(\underline{r};\underline{r}_1)u_{m,n}(\underline{r})\Big\}dv \tag{4.6}$$

We wish to define a situation with an incident unperturbed wave traveling through the uniform isotropic medium characterized by the constant properties ρ and C_{mnps}. The inhomogeneity (the scattering center) characterized by $\Delta\rho$ and ΔC_{mnps} are limited to be contained in a volume V_2, the volume of the scatterer. The Green's function for the uniform medium, given by Eq. (4.2) may be shown to vanish as $|\underline{r}-\underline{r}_1|^{-1}$ as $r_1\to\infty$.. On the infinite surface S, far from the scattering center, the displacement $u_m(\underline{r})$ is just the incident wave $u_m^{(o)}(\underline{r})$. Then

$$u_j^{(o)}(\underline{r}_1) = C_{mnps}\lim_{r\to\infty}\int_S\Big\{G_m^j(\underline{r};\underline{r}_1)u^{(o)}_{s,p}(\underline{r}) - u_m^{(o)}(\underline{r})G^j_{s,p}(\underline{r};\underline{r}_1)\Big\}dS_n \tag{4.7}$$

and hence

$$u_j(\underline{r}_1) = u_j^{(o)}(\underline{r}_1) + \int_{V_2} \Big\{ \Delta\rho(r)\omega^2 G_m^j(\underline{r};\underline{r}_1) u_m(\underline{r}) - \Delta C_{mnps}(\underline{r}) G^j_{s,p}(\underline{r};\underline{r}_1) u_{m,n}(\underline{r}) \Big\} d\underline{r} \quad . \tag{4.8}$$

In an infinite uniform medium $G_m^j(\underline{r};\underline{r}_1)$ can be a function only of the difference $\underline{r}-\underline{r}_1$ (and if the medium is also isotropic, only of the scalar distance $R = |\underline{r}-\underline{r}_1|$). Thus, we can rewrite Eq. (3.13) as

$$G_m^j(\underline{r};\underline{r}_1) = G_j^m(\underline{r}_1;\underline{r}) = G_{jm}(R) = G_{mj}(R) \tag{4.9}$$

where $R = |\underline{r}-\underline{r}_1|$. Equation (4.8) can then be written

$$u_j(\underline{r}) = u_j^{(o)}(\underline{r}) + \int_{V_2} \Big\{ \omega^2 \Delta\rho(\underline{r}') G_{jm}(\underline{r}-\underline{r}') u_m(\underline{r}') + \Delta C_{mnps}(\underline{r}') G_{jm,n}(\underline{r}-\underline{r}') u_{p,s}(\underline{r}') \Big\} d\underline{r}' \tag{4.10}$$

It may shown from Eq. (4.2), for the isotropic medium[5]

$$G_{jm}(R) = \frac{1}{4\pi\rho\omega^2}\left[\left(\kappa^2\delta_{jm} + \frac{\partial^2}{\partial x_j \partial x_m}\right)\frac{e^{-i\kappa R}}{R} - \frac{\partial^2}{\partial x_j \partial x_m}\frac{e^{-ikR}}{R}\right] \tag{4.11}$$

with $\rho\omega^2 = \kappa^2\mu = k^2(\lambda+2\mu)$.

From the solution of Eq. (4.8) one may determine the scattered amplitudes by writing

$$u_j(r) = u_j^{(o)}(r) + u_j^{(s)}(r) \tag{4.12}$$

and the asymptotic expression for $G_{jm}(R)$ for $kR \gg 1$. The scattered wave amplitude, written for $kR \gg 1$, (i.e., the far-field limit) can be expressed as

$$u_m^{(s)}(R) = \frac{1}{R}\left[\Omega_m U^{(\ell)}(\underline{\Omega})e^{-ikR} + (\delta_{jm} - \Omega_j\Omega_m)U_j^{(t)}(\underline{\Omega})e^{-i\kappa R}\right] \tag{4.13}$$

in which $U^{(\ell)}(\underline{\Omega})$ is the amplitude of the longitudinal wave and $U_j^{(t)}(\underline{\Omega})$ that of the transverse wave. These amplitudes are functions of the scattering direction $\underline{\Omega}$, ($\underline{R} = \underline{\Omega}R$), as well as the direction and polarization of the incident wave $u_m^{(o)}(\underline{r})$.

$$U^{(\ell)} = \frac{k^2}{4\pi}\left[\frac{1}{\rho}\int \Omega_j u_j(\underline{r})\Delta\rho(\underline{r})e^{ik\underline{\Omega}\cdot\underline{r}}\,d\underline{r}\right.$$

$$\left. - \frac{i}{(\lambda+2\mu)k}\int [u_{j,j}(\underline{r})\Delta\lambda(\underline{r}) + 2\Delta\mu\Omega_j\Omega_p u_{j,p}(\underline{r})]e^{ik\underline{\Omega}\cdot\underline{r}}\,d\underline{r}\right] \tag{4.14}$$

and

$$U_j^{(t)} = \frac{\kappa^2}{4\pi}\left[\frac{1}{\rho}\int \Delta\rho(\underline{r})u_j(\underline{r})e^{i\kappa\underline{\Omega}\cdot\underline{r}}\,d\underline{r}\right.$$

$$\left. - \frac{i}{\kappa\mu}\Omega_p\int \Delta\mu(\underline{r})[u_{j,p}(\underline{r}) + u_{p,j}(\underline{r})]e^{i\kappa\underline{\Omega}\cdot\underline{r}}\,d\underline{r}\right] \tag{4.15}$$

5. The Born Approximation and the Rayleigh Approximation

One can write equation (4.10) and its derivative in a form which gives a set of coupled integral equations for the displacements and the elastic strains, $\varepsilon_{ij} = \frac{1}{2}(u_{i,j} + u_{j,i})$. Then we have

$$u_j(\underline{r}) = u_j^{(o)}(\underline{r}) + \omega^2 \int \Delta\rho(\underline{r}')G_{jm}(\underline{r}-\underline{r}')u_m(\underline{r}')d\underline{r}' + \int \Delta C_{mnps} G^{(1)}_{j;mn}(\underline{r}-\underline{r}')\varepsilon_{ps}(\underline{r}')dr' \qquad (5.1)$$

where $G^{(1)}_{j;mn}(\underline{R})$ is the symmetrized Green's function derivative,

$$G^{(1)}_{j;mn}(R) = \frac{1}{2}\left[G_{jm,n}(\underline{R}) + G_{jn,m}(\underline{R})\right] \quad .$$

Equation (5.1) is equivalent to (4.10) because of the symmetry of C_{mnps}. From this equation one can now write an equation for ε_{jp} by differentiation but we must include the contribution of the delta-function in $G^{(1)}_{j;mn,s}$. To simplify the notation we now introduce the six-dimensional vector representation for the strains. (The components of the six-dimensional vectors will be designated with Greek subscripts.) We also introduce, for convenience, the dilatation

$$D(\underline{r}) = u_{m,m}(\underline{r}) \equiv \varepsilon_1(\underline{r}) + \varepsilon_2(\underline{r}) + \varepsilon_3(\underline{r}) \qquad (5.2)$$

and write

$$u_j(\underline{r}) = u_j^{(o)}(\underline{r}) + \omega^2 \int \Delta\rho(\underline{r}') G_{jm}(\underline{r}-\underline{r}') u_m(\underline{r}') d\underline{r}'$$
$$+ \int \Delta\lambda(\underline{r}') G_j^{(o)}(\underline{r}-\underline{r}') D(\underline{r}') d\underline{r}'$$
$$+ 2 \int \Delta\mu(\underline{r}') G_{j\beta}^{(1)}(\underline{r}-\underline{r}') \epsilon_\beta(\underline{r}') d\underline{r}' \qquad (5.3a)$$

Differentiating this equation and symmetrizing the resultant expression gives us

$$\epsilon_\alpha(\underline{r}) = \epsilon_\alpha^{(o)}(\underline{r}) + \omega^2 \int \Delta\rho(\underline{r}') G_{\alpha m}^{(2)}(\underline{r}-\underline{r}') u_m(\underline{r}') d\underline{r}'$$
$$+ \int \Delta\lambda(\underline{r}') G_\alpha^{(3)}(\underline{r}-\underline{r}') D(\underline{r}') d\underline{r}'$$
$$+ 2 \int \Delta\mu(\underline{r}') G_{\alpha\beta}^{(4)}(\underline{r}-\underline{r}') \epsilon_\beta(\underline{r}') d\underline{r}' \quad . \qquad (5.3b)$$

where

$$G_j^{(o)}(R) = G_{jm,m}(R) \qquad (5.4a)$$

$$G_{j\beta}^{(1)}(R) = G_{j;pm}^{(1)}(R) \quad , \qquad (5.4b)$$

$$G_{\alpha m}^{(2)}(R) = G_{jp;m}(R) = \frac{1}{2}\left[G_{jm,p}(R) + G_{pm,j}(R)\right] = G_{m;jp}^{(1)}(R) \qquad (5.4c)$$

$$G_\alpha^{(3)}(R) = \frac{1}{2}\left[G_{j,p}^{(o)}(R) + G_{p,j}^{(o)}(R)\right] \qquad (5.4d)$$

$$G_{\alpha\beta}^{(4)}(R) = G_{jp;\beta}^{(4)}(R) = \frac{1}{2}\left[G_{j\beta,p}^{(1)}(R) + G_{p\beta,j}^{(1)}(R)\right] \qquad (5.4e)$$

If we use the incident wave field $u_j^{(o)}$ in equations (4.14) and (4.15) we obtain the Born approximation as it has been developed by Krumhansl, et al.[6]

For incident longitudinal wave $u_j^{(o)} = \frac{K_j}{k} e^{-i\underline{K}\cdot\underline{r}}$ where $\underline{K}$ is the incident wave vector, $K_jK_j = k^2$. Then the scattering angle, θ is given by $\Omega_jK_j = k\cos\theta$ and we have

$$U^{(\ell)} = \frac{k^2}{4\pi}\left[\frac{\Delta\rho}{\rho}\cos\theta - \frac{\Delta\lambda + 2\Delta\mu\cos^2\theta}{\lambda + 2\mu}\right]\int e^{i(k\underline{\Omega}-\underline{K})\cdot\underline{r}}\, d\underline{r} \qquad (5.5a)$$

and

$$U_j^{(t)} = \frac{\kappa^2}{4\pi}\frac{K_j}{k}\left[\frac{\Delta\rho}{\rho} - 2\,\frac{k}{\kappa}\,\frac{\Delta\mu}{\mu}\cos\theta\right]\int e^{i(\kappa\underline{\Omega}-\underline{K})\cdot\underline{r}}\, d\underline{r} \qquad (5.5b)$$

For an incident transverse wave, $u_j^{(o)} = \bar{u}_j e^{-i\underline{K}'\cdot\underline{r}}$ with $|K'| = \kappa$, $\bar{u}_j\bar{u}_j = 1$, and $K'_j\bar{u}_j = 0$, and $\bar{u}_j\Omega_j = \sin\theta\cos\phi$. Then

$$U^{(\ell)} = \frac{k^2}{4\pi}\sin\theta\cos\phi\left[\frac{\Delta\rho}{\rho} - 2\,\frac{k}{\kappa}\,\frac{\Delta\mu}{\mu}\cos\theta\right]\int e^{i(k\underline{\Omega}-\underline{K}')\cdot\underline{r}}\, d\underline{r} \qquad (5.6a)$$

$$U_j^{(t)} = \frac{\kappa^2}{4\pi}\left[\left(\frac{\Delta\rho}{\rho} + \frac{\Delta\mu}{\mu}\cos\theta\right)\bar{u}_j + \frac{K'_j\Delta\mu}{\kappa\mu}\sin\theta\cos\phi\right]\int e^{i(\kappa\underline{\Omega}-\underline{K}')\cdot\underline{r}}\, d\underline{r} \qquad (5.6b)$$

The components parallel and perpendicular to the scattering plane may be found by projection of the vector $\underline{U}^{(t)}$, and one obtains

$$u^{(s)}(t\to t_{\parallel}) = \frac{\kappa^2 e^{-i\kappa R}}{4\pi R}\cos\phi\left[\frac{\Delta\rho}{\rho}\cos\theta + \frac{\Delta\mu}{\mu}\cos 2\theta\right]\int e^{i(\kappa\underline{\Omega}-\underline{K}')\cdot\underline{r}}\, d\underline{r} \qquad (5.7a)$$

$$u^{(s)}(t\to t_{\perp}) = \frac{\kappa^2 e^{-i\kappa R}}{4\pi R}\sin\phi\left[\frac{\Delta\rho}{\rho} + \frac{\Delta\mu}{\mu}\cos\theta\right]\int e^{i(\kappa\underline{\Omega}-\underline{K}')\cdot\underline{r}}\, d\underline{r} \qquad (5.7b)$$

This formulation of the Born approximation is adequate only for the case where $|\Delta\rho| \ll \rho$, $|\Delta\lambda| \ll \lambda$ and $|\Delta\mu| \ll \mu$, otherwise the delta function

contributions from $G_{\alpha}^{(3)}$ and $G_{\alpha\beta}^{(4)}$ in equation (5.3b) cannot be ignored.

In order to identify these delta functions we need look at the Green's function in the limit $\kappa R << 1$ and we write

$$G_{jm}(R) = \frac{1}{8\pi\rho\omega^2}\left[(\kappa^2 + k^2)\frac{\delta_{jm}}{R} + (\kappa^2 - k^2)\frac{x_j x_m}{R^3} + \ldots\right] \tag{5.8}$$

where the omitted terms are finite as R goes to zero. To the same order of approximation we can now evaluate the second order derivatives, but to distinguish the delta function we introduce convergence parameter a and let R^2 be given by $R^2 = x_1^2 + x_2^2 + x_3^2 + a^2 = r^2 + a^2$. After some straightforward algebraic manipulation one finds

$$G_{jm,ps}(R) = \frac{a^2}{8\pi\rho\omega^2 R^7}\left[a^2(\kappa^2 - k^2)\Delta_{jmps} - 2\kappa^2 R^2 \delta_{jm}\delta_{ps} + \ldots\right] \tag{5.9}$$

where Δ_{jmps} is the completely symmetric tensor $\Delta_{jmps} = \delta_{jm}\delta_{ps} + \delta_{jp}\delta_{ms} + \delta_{js}\delta_{pm}$ and in which we have also omitted terms which are spherically anisotropic around the point $\underline{R} = 0$ and for which the integration over angles vanishes. Except for the point r = o it is obvious that equation (5.9) vanishes as a goes to zero. The delta function is then extracted by writing

$$G_{jm,ps}(R) = \frac{\delta(\underline{R})}{2\rho\omega^2}\left[\Delta_{jmps}(\kappa^2 - k^2)J_1 - 2\kappa^2\delta_{jm}\delta_{ps}J_2 + \ldots\right] \tag{5.10}$$

where

$$J_1 = \lim_{a\to o} a^4 \int_o^r \frac{r^2 dr}{R^7} = \int_o^\infty \frac{u^2 du}{(1+u^2)^{7/2}} = \frac{2}{15}$$

$$J_2 = \lim_{a\to o} a^2 \int_o^r \frac{r^2 dr}{R^5} = \int_o^\infty \frac{u^2 du}{(1+u^2)^{5/2}} = \frac{1}{3} \quad .$$

We then obtain

$$G_{jm,ps} = \frac{\delta(\underline{R})}{15\rho\omega^2}\left[(\kappa^2 - k^2)\Delta_{jmps} - 5\kappa^2\delta_{jm}\delta_{ps}\right] + \ldots \tag{5.11}$$

(5.11)

and

$$G_{jp,pm} = -\frac{k^2}{3\rho\omega^2}\,\delta_{jm}\delta(\underline{R}) + \ldots \tag{5.11a}$$

$$G_{jm,pp} - G_{jp,pm} = -\frac{2\kappa^2}{3\rho\omega^2}\,\delta_{jm}\delta(\underline{R}) + \ldots \tag{5.11b}$$

These expressions satisfy the delta-function component of equation (4.2). We note that the omitted terms in equation (5.11) may and indeed do contain singularities of order R^{-1} but these lead to finite contributions to the integrals in (5.3b). The singificant feature of the delta-function contributions in equation (5.3b) is that they are independent of the geometry of the scatterer. Equation (5.3b) may then be written in the form

$$\begin{aligned}\epsilon_\alpha(\underline{r}) = \epsilon_\alpha^{(o)}(\underline{r}) - A_{\alpha\beta}\epsilon_\beta(\underline{r}) + \omega^2 \int \Delta\rho(\underline{r}')\, G_{\alpha m}^{(2)}(|\underline{r}-\underline{r}'|)u_m(\underline{r}')d\underline{r}' \\ + \int \Delta\lambda(\underline{r}')G_\alpha^{(3)}(|\underline{r}-\underline{r}'|)D(\underline{r}')d\underline{r}' \\ + 2\int \Delta\mu(\underline{r}')\tilde{G}_{\alpha\beta}^{(4)}(|\underline{r}-\underline{r}'|)\epsilon_\beta(\underline{r}')d\underline{r}'\end{aligned} \tag{5.12}$$

where $A_{\alpha\beta}(\underline{r})$ is the contribution of the delta functions and $\tilde{G}^{(3)}_{\alpha}(R)$ and $\tilde{G}^{(4)}_{\alpha\beta}(R)$ are the regular (i.e., delta-function-free) parts of the Green's function. We now let S denote the "shielding" matrix which is the inverse of $\delta_{\alpha\beta} + A_{\alpha\beta}(\underline{r})$ and write

$$\varepsilon_{\alpha}(\underline{r}) = S_{\alpha\gamma}(\underline{r})\Big[\varepsilon^{(o)}_{\gamma}(\underline{r}) + \omega^2\int\Delta\rho(\underline{r}')G^{(2)}_{\gamma m}(\underline{r}-\underline{r}')u_m(\underline{r}')d\underline{r}'$$

$$+\int\Delta\lambda(\underline{r}')\tilde{G}^{(3)}_{\gamma}(|\underline{r}-\underline{r}'|)D(\underline{r}')d\underline{r}'$$

$$+ 2\int\Delta\mu(\underline{r}')\tilde{G}^{(4)}_{\gamma\beta}(|\underline{r}-\underline{r}'|)\varepsilon_{\beta}(\underline{r}')d\underline{r}'\Big] \qquad (5.12a)$$

Our "corrected" Born approximation involves dropping the contributions of the integrals in this equation and using as our first approximation the "shielded" strain field

$$\varepsilon_{\alpha}(\underline{r}) = S_{\alpha\gamma}(\underline{r})\varepsilon^{(o)}_{\gamma}(\underline{r}) \qquad (5.12b)$$

in equations (4.14a-b) to calculate the scattered amplitudes.

There is in fact no need to evaluate the matrix $S(\underline{r})$; it has already been evaluated in the exact solution of the spherical scatterer. In lowest order the shielding matrix can be extracted from the Rayleigh limit in the spherical problem. Since $S(\underline{r})$ is geometry-independent, the Rayleigh limit can then be converted into the Born approximation when one expresses the scattering amplitudes in the form

$$u^{(s)}_{j}(\underline{R}) \sim \frac{k^2a^3}{3} f(R,\underline{\Omega},\underline{K}) \quad .$$

It is clear that $a^3/3$ for the sphere is simply $V/4\pi$ and hence should be replaced by the appropriate Fourier transform integral; e.g., $a^3/3 \rightarrow \frac{1}{4\pi} \int e^{i(k\underline{\Omega}-\underline{K})\cdot\underline{r}}\, d\underline{r}$ in equation (5.5a).

We have omitted some terms in evaluating the delta-function contributions in equations (5.3a,b) arising from the spatial derivatives of the elastic constants, which, even for a scattering volume of constant properties, will not vanish because of the step jump in properties at the surface. This will introduce a surface integral into the shielding matrix $A_{\alpha\beta}$ in equation (5.12). Such a term is to be expected because the shielding must depend on both the shape and the orientation of the scattering object. Such effects are well known in both the static elasticity problem and in the analogous scattering of electromagnetic radiation. For a spherical scatterer these terms can be exactly included by using the Rayleigh limit of the exact calculation to evaluate the shielding factor. For non-spherical scatterers, however, equation (5.12a) is incomplete and is appropriate only for shapes which differ only slightly from spherical. It is expected that the complete identification of all of the delta-functions in equations (5.3a) and (5.3b) will yield a significantly improved formulation that will allow the Born approximation to provide an appropriate first approximation to scattering by such extremely non-spherical defects as cracks or discs.

Using the Rayleigh limit for the exact solution to the problem of the spherical scatterer allows us to define a surprisingly simple correction to the Born approximation.

We define the coefficients

$$A_o = \frac{\Delta\lambda + \frac{2}{3}\Delta\mu}{\lambda + 2\mu + \Delta\lambda + \frac{2}{3}\Delta\mu} \quad ; \quad A_2 = \frac{\Delta\mu}{\mu + \frac{2}{15}(3 + 2k^2/\kappa^2)\Delta\mu} \quad .$$

We then obtain, for the scattered wave amplitudes with incident compressional waves

$$u^{(s)}_{(\ell\to\ell)} = \frac{k^2 e^{-ikR}}{4\pi R}\left[\frac{\Delta\rho}{\rho}\cos\theta - A_o - \frac{2k^2}{\kappa^2}A_2(\cos^2\theta - \frac{1}{3})\right]\int e^{i(k\underline{\Omega}-\underline{K})\cdot\underline{r}}\, d\underline{r} \tag{5.13a}$$

$$u^{(s)}_{(\ell\to t)} = \frac{\kappa^2 e^{-i\kappa R}}{4\pi R}\left[\frac{\Delta\rho}{\rho} - \frac{2k}{\kappa}A_2\cos\theta\right]\sin\theta\int e^{i(\kappa\underline{\Omega}-\underline{K})\cdot\underline{r}}\, d\underline{r} \tag{5.13b}$$

We note that in this approximation the scattered transverse wave is polarized in the scattering plane. For a scatterer with axial symmetry around the axis of the incident wave vector this would follow from simple symmetry arguments. The implication here is that for an arbitrary shape the out-of-plane polarization amplitude is geometry-dependent and hence of order $\kappa^2 V^{2/3}\varepsilon$ (where ε is a measure of the asymmetry) smaller than the in-plane amplitude.

For the scattered wave amplitudes with incident shear waves we obtain

$$u^{(s)}_{(t\to\ell)} = \frac{k^2 e^{-ikR}}{4\pi R}\sin\theta\cos\phi\left[\frac{\Delta\rho}{\rho} - \frac{2k}{\kappa}A_2\cos\theta\right]\int e^{i(k\underline{\Omega}-\underline{K})\cdot\underline{r}}\, d\underline{r} \tag{5.14a}$$

$$u^{(s)}_{(t\to t_{\parallel})} = \frac{\kappa^2 e^{-i\kappa R}}{4\pi R}\cos\phi\left[\frac{\Delta\rho}{\rho}\cos\theta - A_2(2\cos^2\theta - 1)\right]e^{i(\kappa\underline{\Omega}-\underline{K})\cdot\underline{r}}\, d\underline{r} \tag{5.14b}$$

$$u^{(s)}_{(t\to t_{\perp})} = \frac{\kappa^2 e^{-i\kappa R}}{4\pi R}\sin\phi\left[\frac{\Delta\rho}{\rho} - A_2\cos\theta\right]\int e^{i(\kappa\underline{\Omega}-\underline{K})\cdot\underline{r}}\, d\underline{r} \quad . \tag{5.14c}$$

The comparison of the first order Born approximation (equations (5.5a (5.6a), and (5.7a,b)) and the corrected Born approximation (equations (5.13a,b) and (5.14a,b,c)) with the exact calculations for the scattering from a WC inclusion in Ti alloy is shown in Figs. 9-12. It is clear that in this case in which we have $\Delta\rho/\rho = 2.1$, $\Delta\lambda/\lambda = 0.8$ and $\Delta\mu/\mu = 4.4$ the "shielding" effect should be quite important. As expected for a situation with κa not small, ($\kappa a = 1.87$) the Born approximation is not too good, particularly in the forward scattering direction. The corrected Born approximation is significantly better.

III. PUBLICATIONS AND PRESENTATIONS

Presentations

1. B. R. Tittmann, "Mode Conversion and Angular Dependence for Scattering from Voids in Solids," IEEE Ultrasonics Symposium, Los Angeles, 1975, N-5.
2. B. R. Tittmann, "Elastic Wave Scattering from Spherical Cavities," Acoust. Soc. America, 90th Meeting, San Francisco, 1975, III-5.

Publications

1. E. Richard Cohen and B. R. Tittmann, "Analysis of Ultrasonic Wave Scattering for Characterization of Defects in Solids," Science Center, Rockwell International, Technical Report, SCTR-75-12 (December, 1975).
2. B. R. Tittmann, "Mode Conversion and Angular Dependence for Scattering from Voids in Solids," Ultrasonics Symposium Proc., IEE Cat. #75 CH0994-4SU, p. 111 (1975).
3. B. R. Tittmann and E. Richard Cohen, "Scattering of Longitudinal Waves Incident on a Cavity in a Solid," J. Acoustical Soc. Amer. (submitted).
4. E. Richard Cohen, "Analysis of Ultrasonic Scattering from Simply Shaped Objects," Proc. ARPA/AFML Review of Quantitative NDE, Science Center, Rockwell International (1975).
5. B. R. Tittmann, J. M. Richardson, and E. R. Cohen, "Ultrasonic Scattering Measurements in Solids Using Short Broadband Pulses," J. Acoust. Soc. Amer. (submitted). (Support partially from ARPA/AFML F33615-74-C-5180)
6. B. R. Tittmann and E. R. Cohen, "Scattering of Transverse Waves Incident on a Cavity in a Solid," (in preparation).
7. B. R. Tittmann and E. R. Cohen, "Scattering of Ultrasonic Waves from a Spherical Inclusion in a Solid," (in preparation).

IV. REFERENCES

1. E. Richard Cohen, "Analysis of Ultrasonic Wave Scattering for Characterization of Defects in Solids," First Annual Interim Report. SC579.1IR, Science Center, Rockwell International, March 1975.
2. B. R. Tittmann, J. M. Richardson, and E. Richard Cohen, "Ultrasonic Scattering Measurements in Solids Using Short Broadband Pulses," J. Acoust. Soc. Am. (submitted for publication).
3. E. Richard Cohen and B. R. Tittmann, "Analysis of Ultrasonic Wave Scattering for the Characterization of Defects in Solids," Science Center, Rockwell International, Technical Report SCTR-75-12 (December 1975).
4. Leon Knopoff and A. F. Gangi, "Seismic Reciprocity," Geophysics XXIV, 681 (October 1959).
5. We note that P. M. Morse, "Vibrations of Elastic Bodies," Part 3, Chap. 7 of Handbook of Chemistry and Physics, edited by E. U. Condon and H. Odishaw (McGraw-Hill, 2nd Edition, 1967) pp. 3-101, and P. M. Morse and H. Feshbach, Methods of Theoretical Physics (McGraw-Hill, New York, 1953) give an incorrect expression for $G_{jm}(R)$. These authors also use $e^{-i\omega t}$ for the time dependence. We use $e^{i\omega t}$ for the time dependence in this analysis.
6. J. A. Krumhansl, Proceedings of the ARPA/AFML Review of Quantitative NDE, December 5, 1975, p. 57.

Figure Captions

Fig. 1 Frequency analysis of the transmitted pulses using nominal 2.25 MHz, 5.0 MHz and 10 MHz broadband transducers.

Fig. 2 Scattering distributions for incident compressional waves; 2.25 MHz.

Fig. 3 Scattering distributions for incident compressional waves; 5.0 MHz.

Fig. 4 Scattering distributions for incident compressional waves; 10 MHz.

Fig. 5 Scattering distributions for incident shear waves; 2.5 MHz.

Fig. 6 Scattering distributions for incident shear waves; 5.0 MHz.

Fig. 7 Scattering distributions for incident shear waves; 10.0 MHz.

Fig. 8 Reciprocity in scattering of acoustic waves.

Fig. 9 Comparison of Born approximations: Direct scattering, Incident compressional wave. ka = 0.89, WC sphere in Ti64. ——, exact solution; ····, lowest order Born approximation; ---, shielded Born approximation.

Fig. 10 Comparison of Born approximations: Mode conversion, longitudinal to transverse or vice versa, ka = 0.89; κa = 1.87; WC sphere in Ti64. ——, exact solution; ····, lowest order Born approximation; ---, shielded Born approximation.

Fig. 11 Comparison of Born approximations: Parallel scattered shear wave, κa = 1.87; WC sphere in Ti64. ——, exact solution; ····, lowest order Born approximation; ---, shielded Born approximation.

Fig. 12 Comparison of Born approximations: Perpendicularly scattered shear wave, κa = 1.87; WC sphere in Ti64. ——, exact solution; ····, lowest order Born approximation; ---, shielded Born approximation.

Figure Captions

Fig. 1 Frequency analysis of the transmitted pulses using nominal 2.25 MHz, 5.0 MHz and 10 MHz broadband transducers.

Fig. 2 Scattering distributions for incident compressional waves; 2.25 MHz.

Fig. 3 Scattering distributions for incident compressional waves; 5.0 MHz.

Fig. 4 Scattering distributions for incident compressional waves; 10 MHz.

Fig. 5 Scattering distributions for incident shear waves; 2.5 MHz.

Fig. 6 Scattering distributions for incident shear waves; 5.0 MHz.

Fig. 7 Scattering distributions for incident shear waves; 10.0 MHz.

Fig. 8 Reciprocity in scattering of acoustic waves.

Fig. 9 Comparison of Born approximations: Direct scattering, Incident compressional wave. $ka = 0.89$, WC sphere in Ti64. ——, exact solution; ····, lowest order Born approximation; ---, shielded Born approximation.

Fig. 10 Comparison of Born approximations: Mode conversion, longitudinal to transverse or vice versa, $ka = 0.89$; $\kappa a = 1.87$; WC sphere in Ti64. ——, exact solution; ····, lowest order Born approximation; ---, shielded Born approximation.

Fig. 11 Comparison of Born approximations: Parallel scattered shear wave, $\kappa a = 1.87$; WC sphere in Ti64. ——, exact solution; ····, lowest order Born approximation; ---, shielded Born approximation.

Fig. 12 Comparison of Born approximations: Perpendicularly scattered shear wave, $\kappa a = 1.87$; WC sphere in Ti64. ——, exact solution; ····, lowest order Born approximation; ---, shielded Born approximation.

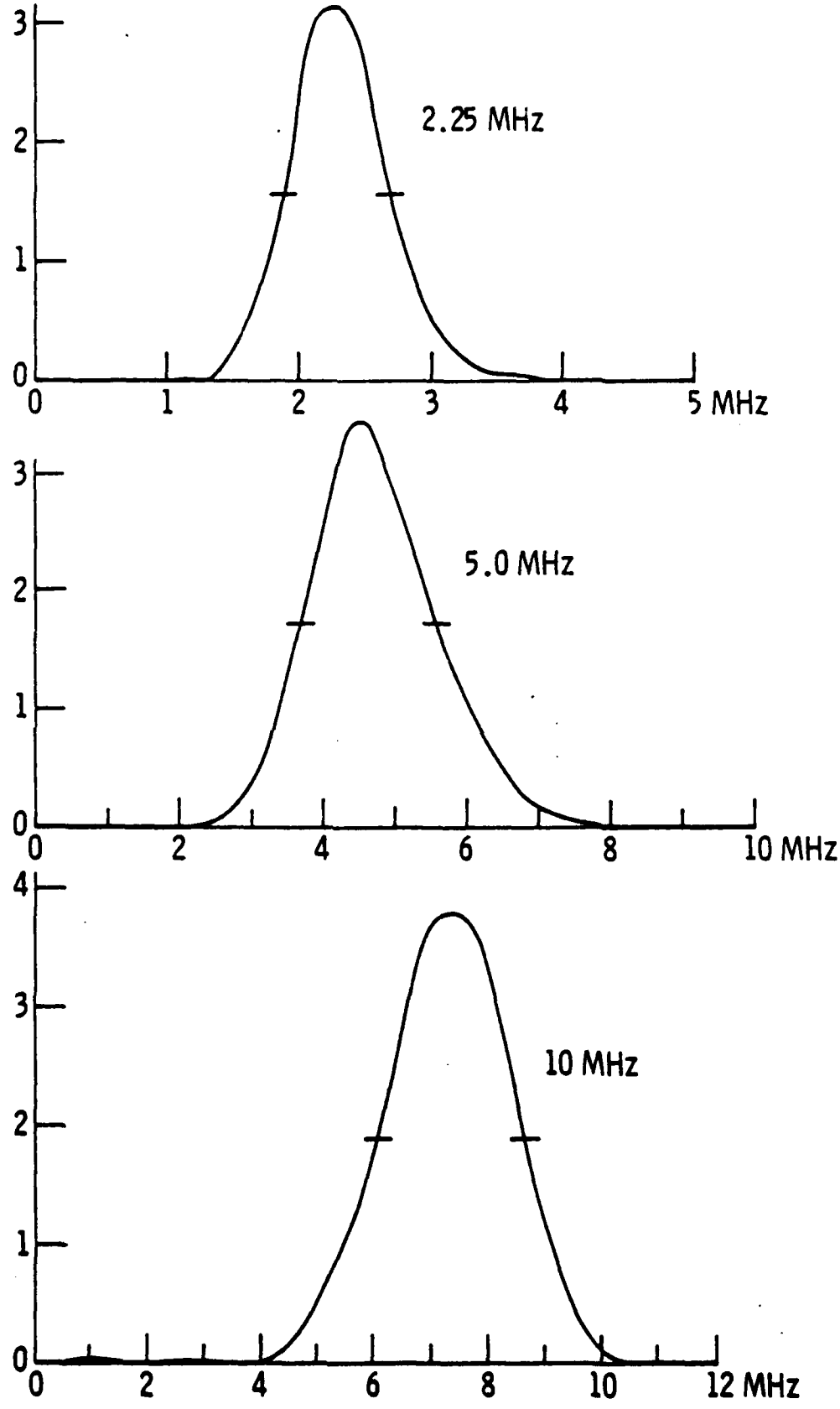

Fig. 1

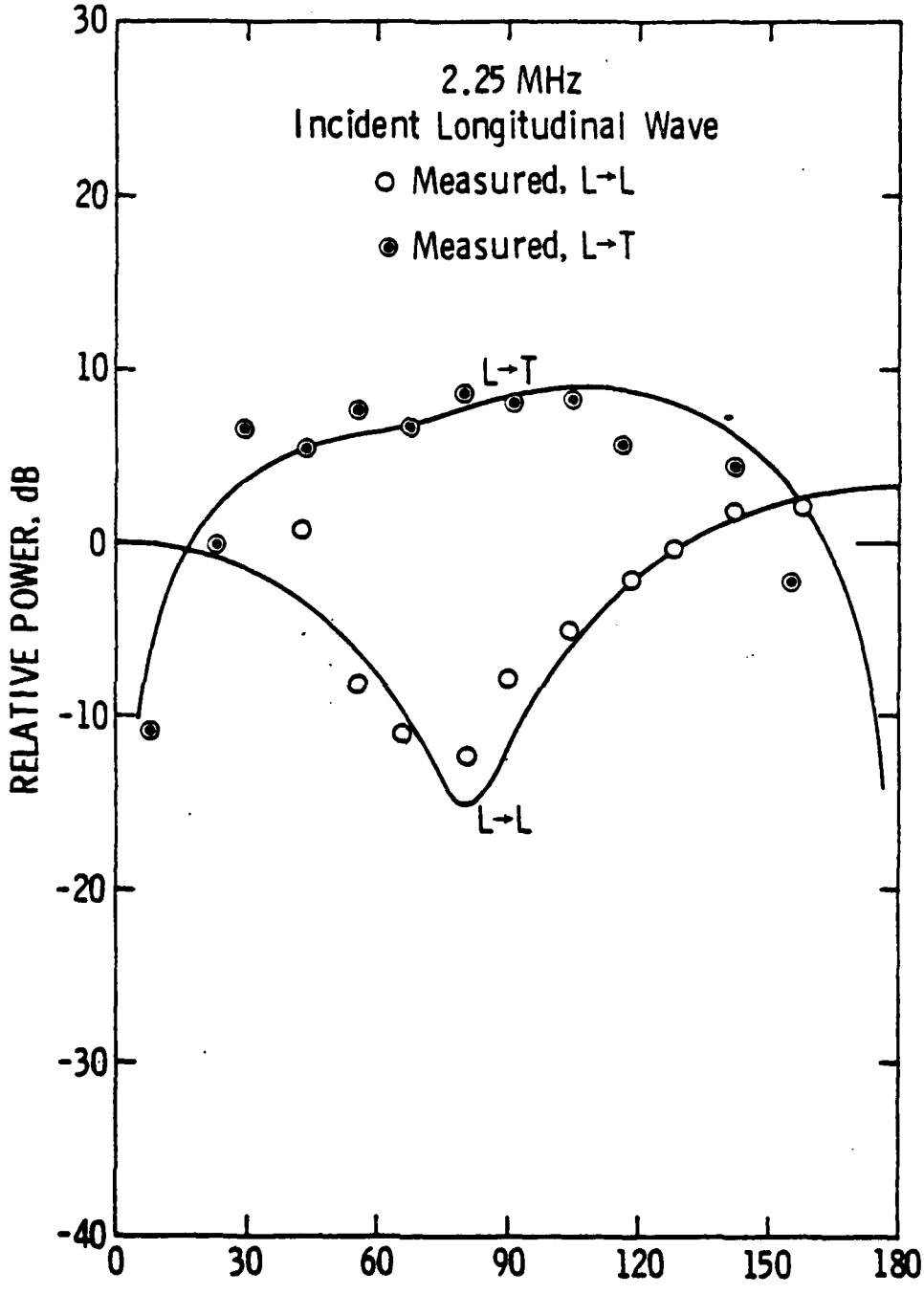
2.25 MHz
Incident Longitudinal Wave
Measured, L→L
Measured, L→T
L→T
L→L
RELATIVE POWER, dB
30
20
10
0
-10
-20
-30
-40
0
30
60
90
120
150
180

Fig. 2

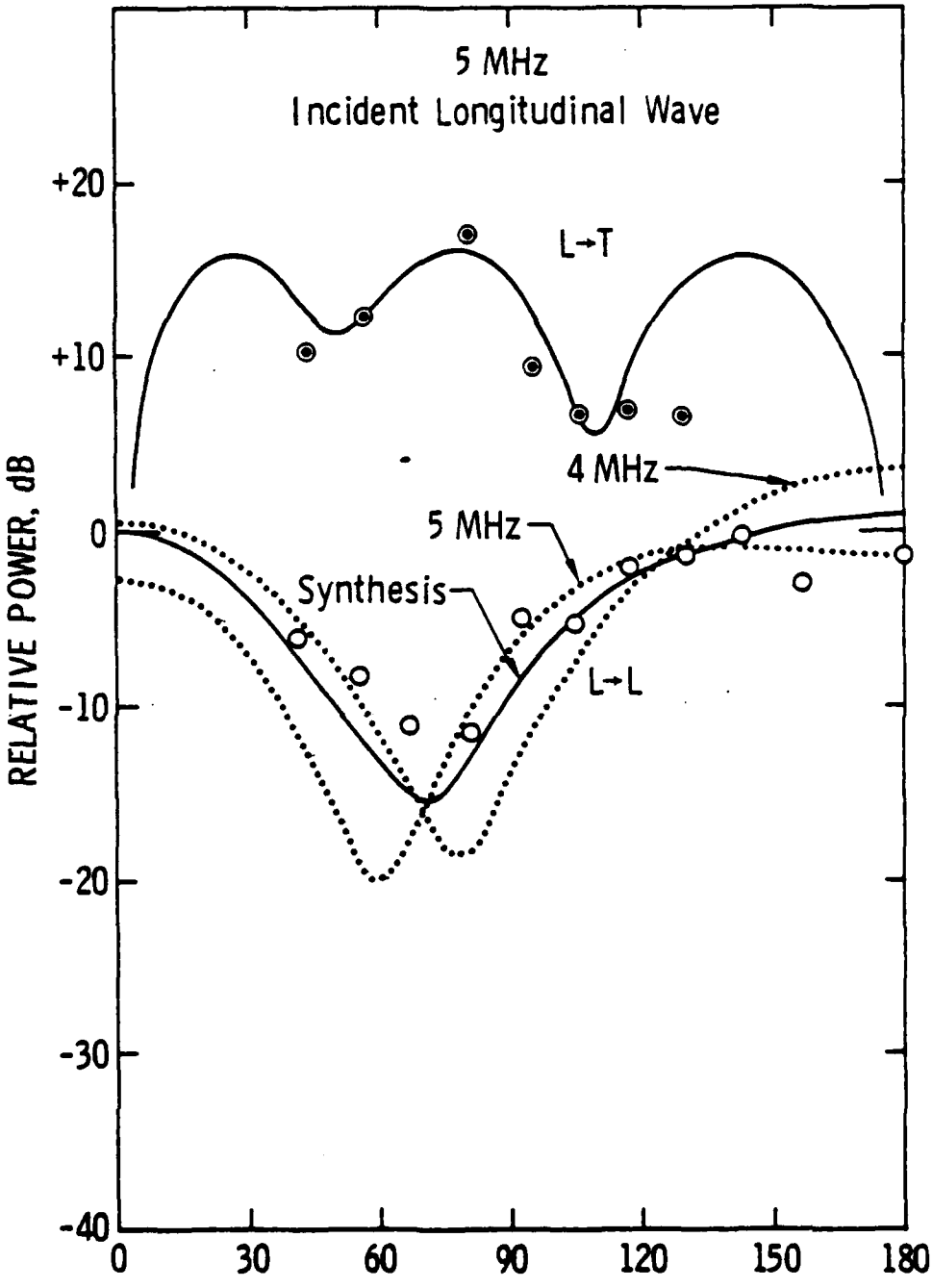
5 MHz
Incident Longitudinal Wave
+20
+10
0
-10
-20
-30
-40
RELATIVE POWER, dB
0
30
60
90
120
150
180
L→T
4 MHz
5 MHz
Synthesis
L→L

Fig. 3

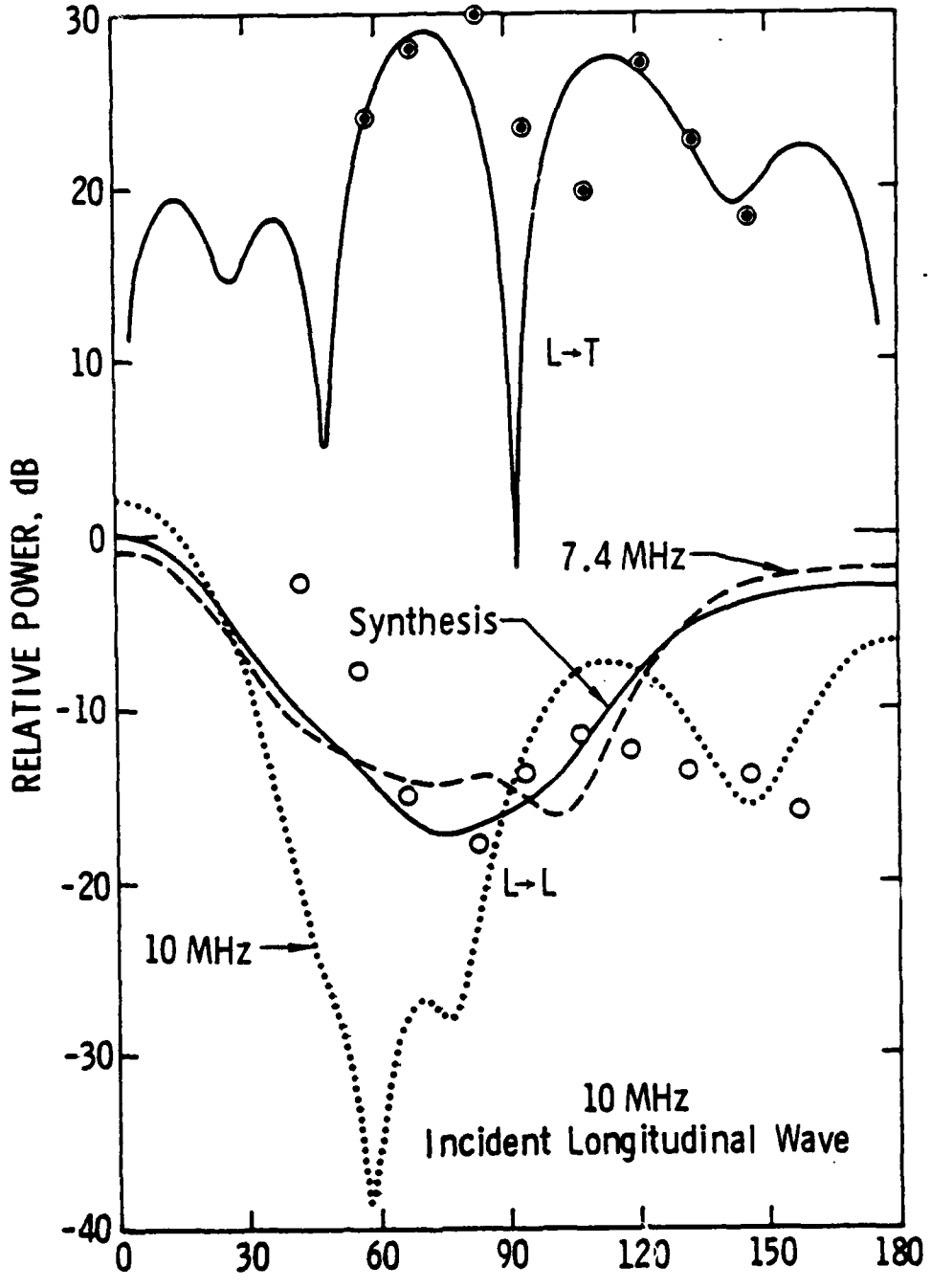
30
20
10
0
-10
-20
-30
-40
0
30
60
90
120
150
180
RELATIVE POWER, dB
L→T
7.4 MHz
Synthesis
L→L
10 MHz
10 MHz
Incident Longitudinal Wave

Fig. 4

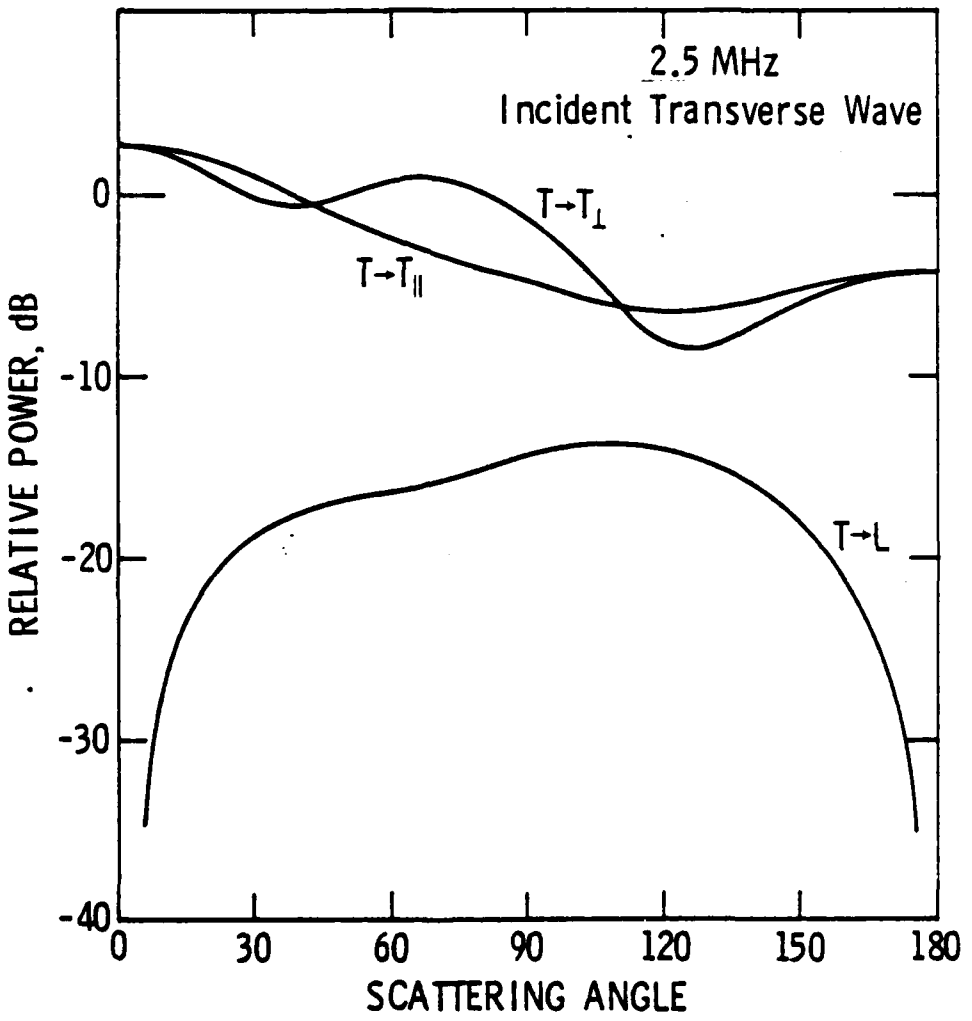
2.5 MHz
Incident Transverse Wave
T→T⊥
T→T∥
T→L
RELATIVE POWER, dB
0
-10
-20
-30
-40
0
30
60
90
120
150
180
SCATTERING ANGLE

Fig. 5

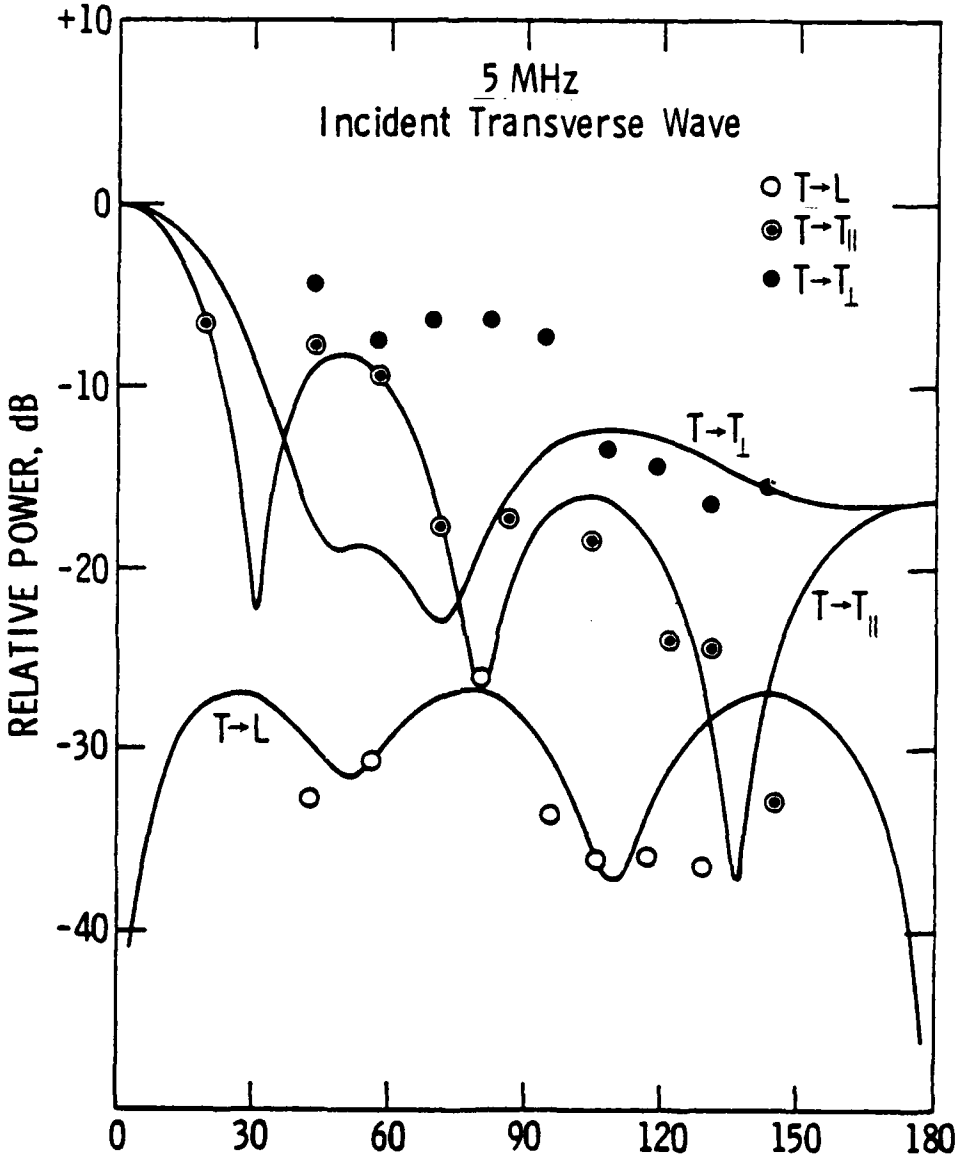
5 MHz
Incident Transverse Wave
T→L
T→T∥
T→T⊥
RELATIVE POWER, dB
+10
0
-10
-20
-30
-40
0
30
60
90
120
150
180

Fig. 6

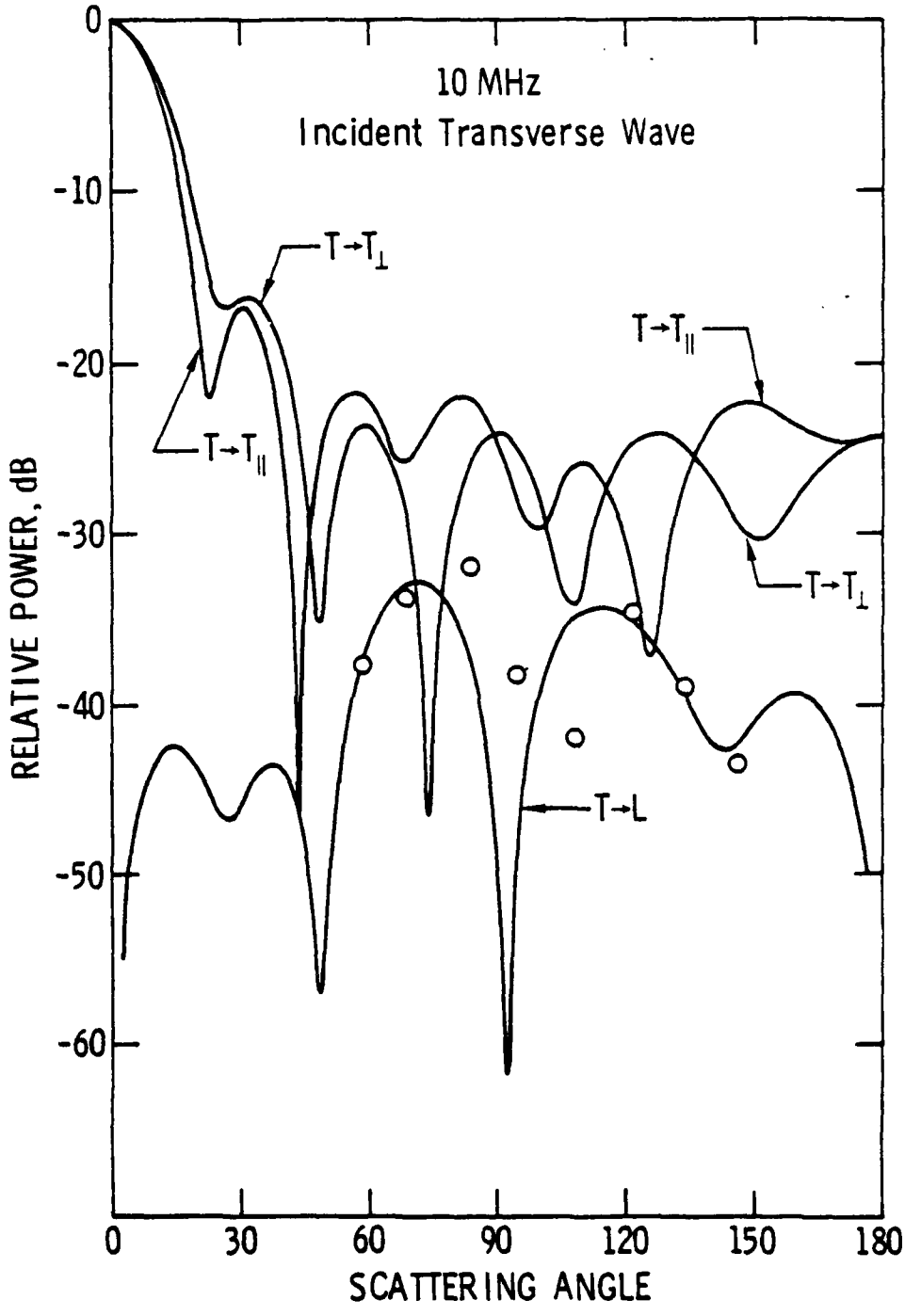
10 MHz
Incident Transverse Wave
T→T⊥
T→T∥
T→T∥
T→T⊥
T→L
RELATIVE POWER, dB
SCATTERING ANGLE
0
-10
-20
-30
-40
-50
-60
0
30
60
90
120
150
180

Fig. 7

Fig. 8

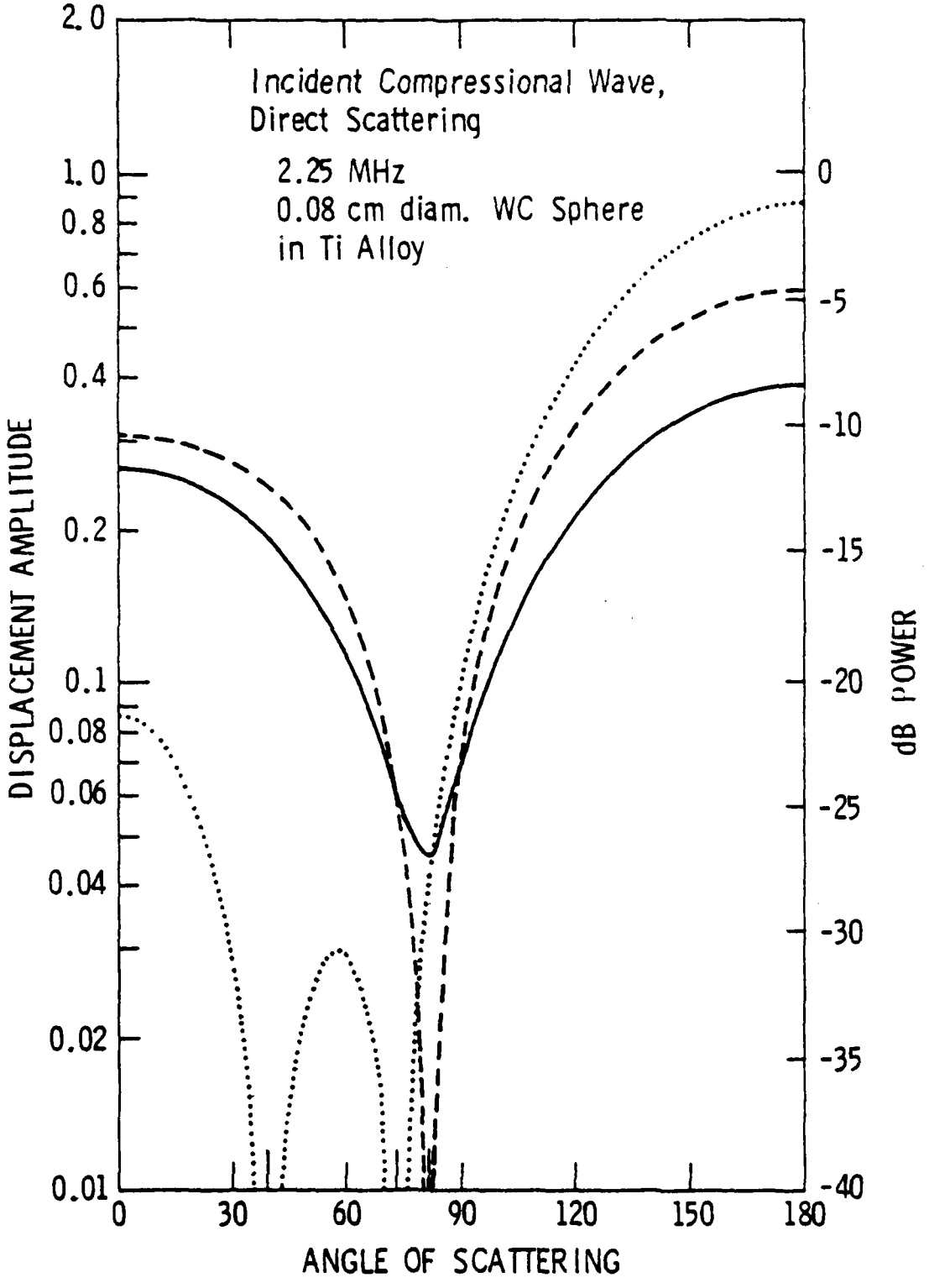
Incident Compressional Wave,
Direct Scattering
2.25 MHz
0.08 cm diam. WC Sphere
in Ti Alloy
DISPLACEMENT AMPLITUDE
dB POWER
ANGLE OF SCATTERING
2.0
1.0
0.8
0.6
0.4
0.2
0.1
0.08
0.06
0.04
0.02
0.01
0
-5
-10
-15
-20
-25
-30
-35
-40
0
30
60
90
120
150
180

Fig. 9

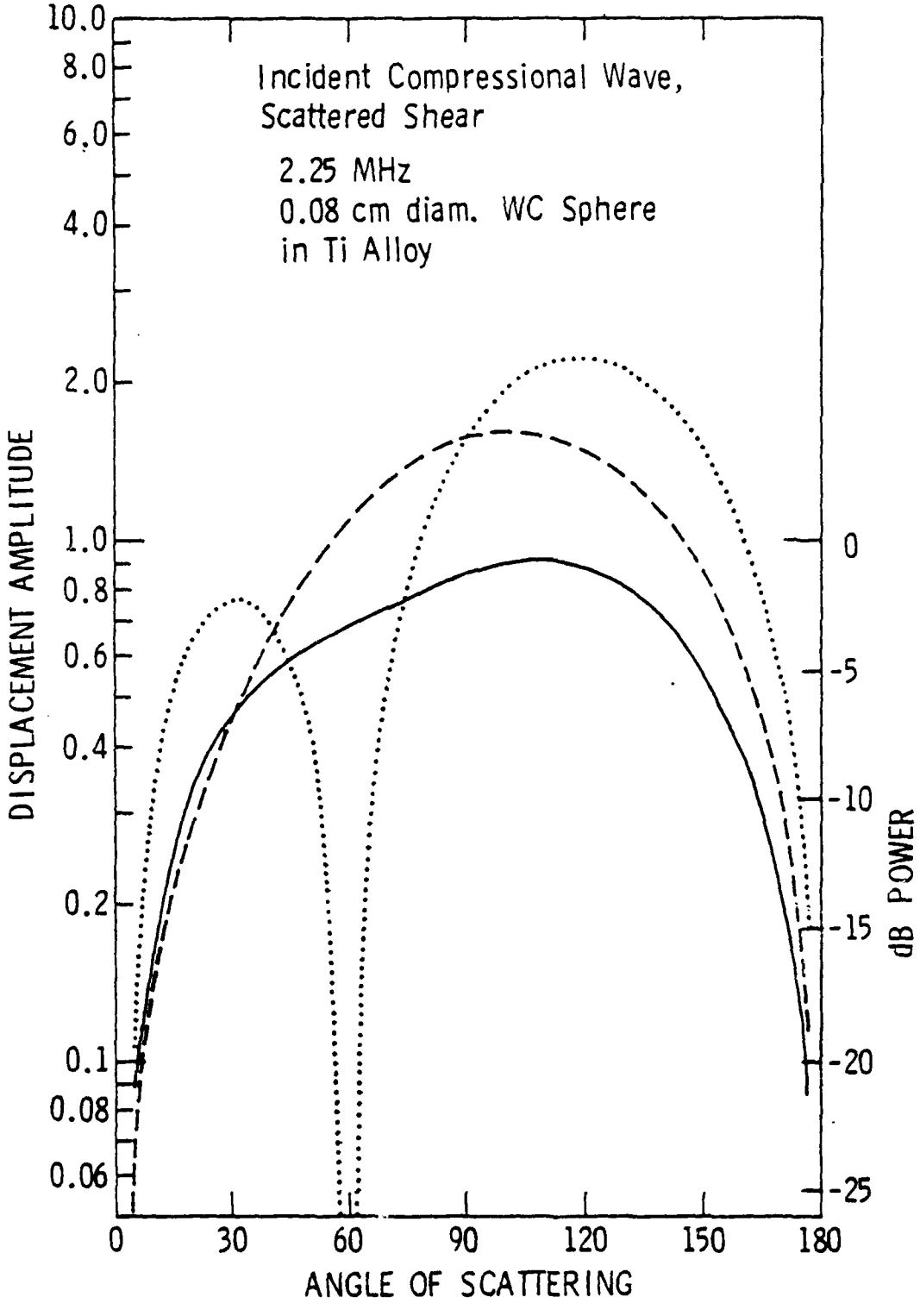
Incident Compressional Wave,
Scattered Shear
2.25 MHz
0.08 cm diam. WC Sphere
in Ti Alloy
DISPLACEMENT AMPLITUDE
10.0
8.0
6.0
4.0
2.0
1.0
0.8
0.6
0.4
0.2
0.1
0.08
0.06
dB POWER
0
-5
-10
-15
-20
-25
0
30
60
90
120
150
180
ANGLE OF SCATTERING

Fig. 10

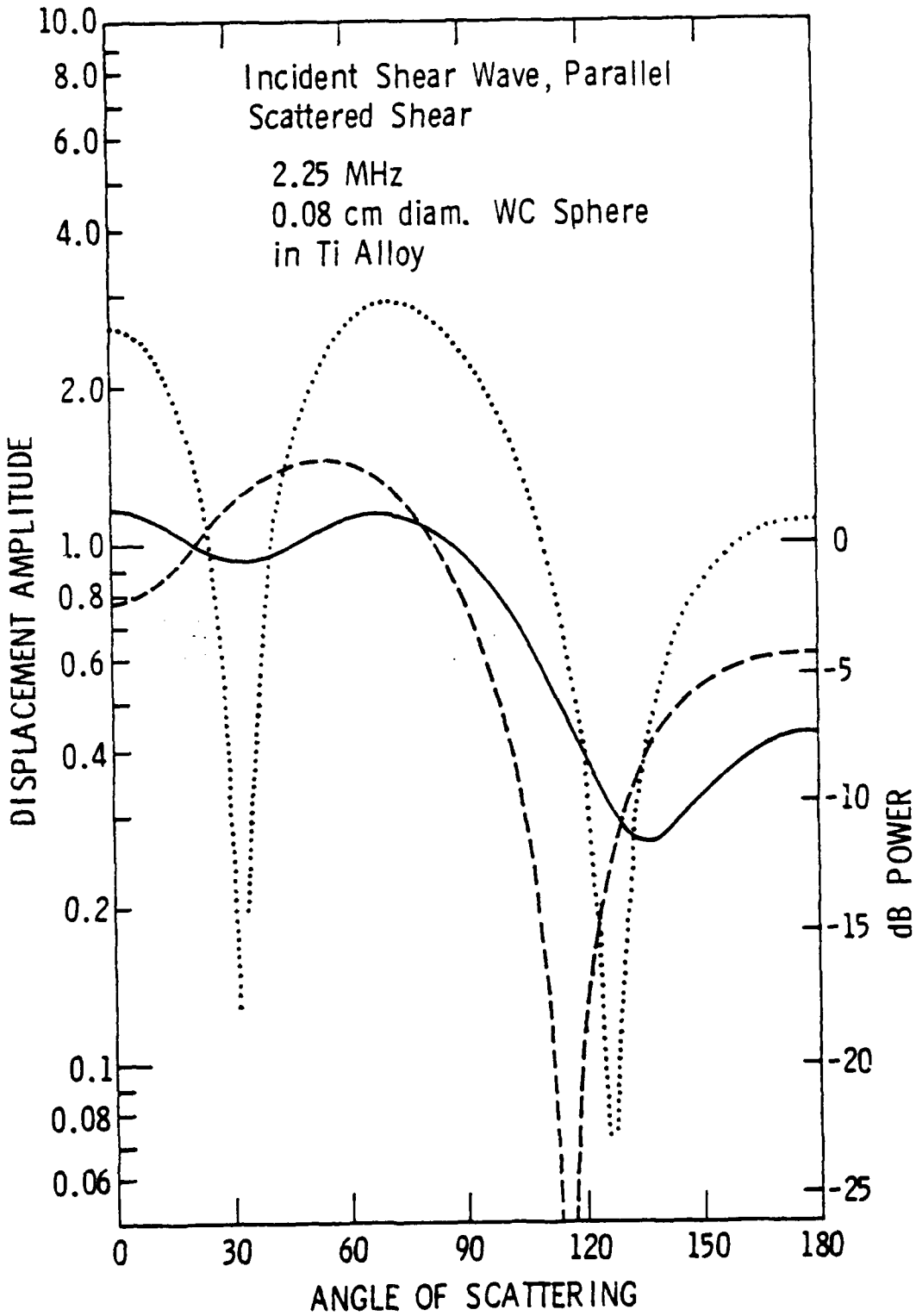
Incident Shear Wave, Parallel
Scattered Shear
2.25 MHz
0.08 cm diam. WC Sphere
in Ti Alloy
DISPLACEMENT AMPLITUDE
10.0
8.0
6.0
4.0
2.0
1.0
0.8
0.6
0.4
0.2
0.1
0.08
0.06
dB POWER
0
-5
-10
-15
-20
-25
0
30
60
90
120
150
180
ANGLE OF SCATTERING

Fig. 11

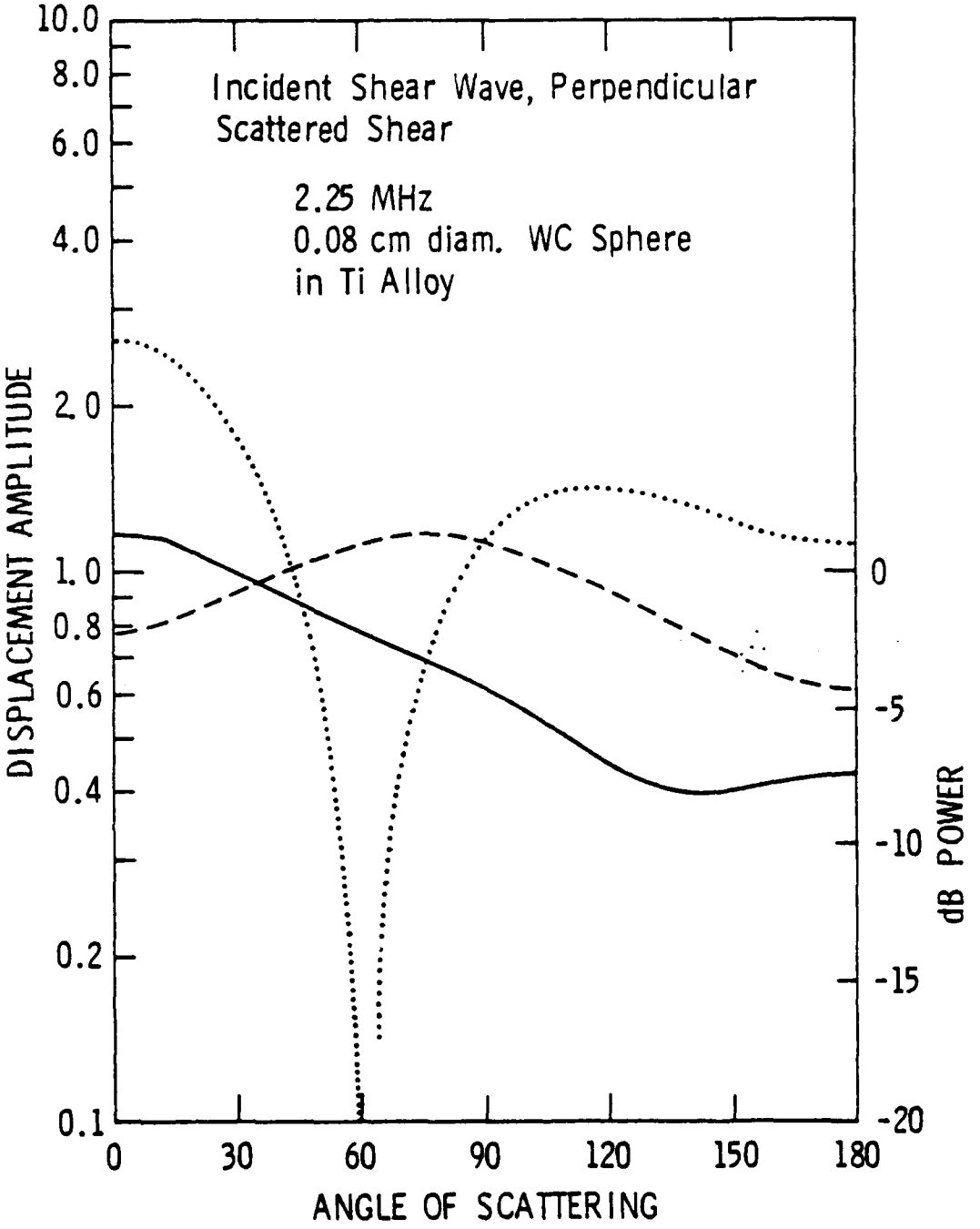
Incident Shear Wave, Perpendicular
Scattered Shear
2.25 MHz
0.08 cm diam. WC Sphere
in Ti Alloy
DISPLACEMENT AMPLITUDE
10.0
8.0
6.0
4.0
2.0
1.0
0.8
0.6
0.4
0.2
0.1
dB POWER
0
-5
-10
-15
-20
0
30
60
90
120
150
180
ANGLE OF SCATTERING

Fig. 12